Prophylactic Knockdown of the miR-183/96/182 Cluster Ameliorates *Pseudomonas aeruginosa*–Induced Keratitis

Sharon McClellan,[1] Ahalya Pitchaikannu,[1] Robert Wright,[1] Denise Bessert,[1] Mason Iulianelli,[2] Linda D. Hazlett,[1] and Shunbin Xu[1]

[1]Department of Ophthalmology, Visual and Anatomical Sciences, School of Medicine, Wayne State University, Detroit, Michigan, United States
[2]Departments of Biological Sciences and Public Health, College of Liberal Arts and Sciences, Wayne State University, Detroit, Michigan, United States

Correspondence: Shunbin Xu, Department of Ophthalmology, Visual and Anatomical Sciences, School of Medicine, Wayne State University, 540 E. Canfield Avenue, Detroit, MI 48201, USA; sxu@med.wayne.edu.

Received: March 25, 2021
Accepted: November 3, 2021
Published: December 17, 2021

Citation: McClellan S, Pitchaikannu A, Wright R, et al. Prophylactic knockdown of the miR-183/96/182 cluster ameliorates *Pseudomonas aeruginosa*–induced keratitis. *Invest Ophthalmol Vis Sci.* 2021;62(15):14. https://doi.org/10.1167/iovs.62.15.14

Purpose. Previously, we demonstrated that miR-183/96/182 cluster (miR-183C) knockout mice exhibit decreased severity of *Pseudomonas aeruginosa* (PA)-induced keratitis. This study tests the hypothesis that prophylactic knockdown of miR-183C ameliorates PA keratitis indicative of a therapeutic potential.

Methods. Eight-week-old miR-183C wild-type and C57BL/6J inbred mice were used. Locked nucleic acid–modified anti-miR-183C or negative control oligoribonucleotides with scrambled sequences (NC ORNs) were injected subconjunctivally 1 day before and then topically applied once daily for 5 days post-infection (dpi) (strain 19660). Corneal disease was graded at 1, 3, and 5 dpi. Corneas were harvested for RT-PCR, ELISA, immunofluorescence (IF), myeloperoxidase and plate count assays, and flow cytometry. Corneal nerve density was evaluated in flatmounted corneas by IF staining with anti-β-III tubulin antibody.

Results. Anti-miR-183C downregulated miR-183C in the cornea. It resulted in an increase in IL-1β at 1 dpi, which was decreased at 5 dpi; fewer polymorphonuclear leukocytes (PMNs) at 5 dpi; lower viable bacterial plate count at both 1 and 5 dpi; increased percentages of MHCII$^+$ macrophages (Mϕ) and dendritic cells (DCs), consistent with enhanced activation/maturation; and decreased severity of PA keratitis. Anti-miR-183C treatment in the cornea of naïve mice resulted in a transient reduction of corneal nerve density, which was fully recovered one week after the last anti-miR application. miR-183C targets repulsive axon-guidance receptor molecule Neuropilin 1, which may mediate the effect of anti-miR-183C on corneal nerve regression.

Conclusions. Prophylactic miR-183C knockdown is protective against PA keratitis through its regulation of innate immunity, corneal innervation, and neuroimmune interactions.

Keywords: microRNA, *Pseudomonas aeruginosa*, keratitis, miR-183/96/182 cluster (miR-183C), inflammation, neuroimmune interaction

MicroRNAs (miRNAs) are small, non-coding regulatory RNAs, ~20 to 24 nucleotides in size.[1–4] MiRNAs constitute an important post-transcriptional regulation of gene expression. A mature miRNA regulates its downstream target genes by base pairing with the target sites in their transcripts, typically in the 3′ untranslated region,[2,5] inducing either mRNA breakdown or translational inhibition. MiRNAs function in a cell type–specific manner. One miRNA often quantitatively regulates groups of genes that are involved in the same or related functional pathways or networks.[6–11] Modest regulation of multiple genes in concert imposes significant functional consequences on the signaling pathway or network.[6–9] MiRNAs have been proven to play important roles in normal tissue development and functions, as well as in the pathogenesis of diseases.[12–14] Various approaches have been developed to enhance or knock down the functions of miRNAs in vivo.[15–17] Synthetic oligoribonucleotides (ORNs) that mimic the native miRNA duplex are used to enhance the function of a miRNA[18]; single-stranded antisense ORNs are used to sequester an endogenous miRNA of interest to inhibit its function. A variety of chemical modifications of the ORNs, such as 2′-*O*-methoxyethyl (2′-MOE) and locked nucleic acid (LNA) bases, have been developed to enhance RNA stability for in vivo applications.[15,19] Several clinical trials targeting miRNAs (e.g., miR-34, miR-16) are ongoing to test their safety in cancer treatment.[20]

In spite of their important roles in health and disease, our knowledge about miRNAs and their potential in the treatment of ocular infectious diseases is still limited. Previously, we demonstrated that a conserved miRNA cluster, the miR-183/96/182 cluster (miR-183C), plays a significant role in modulating the corneal response to *Pseudomonas aeruginosa* (PA) infection. PA is a Gram-negative opportunistic pathogen capable of inducing keratitis. PA keratitis is one

of the most rapidly developing and destructive diseases of the cornea,[21,22] and PA remains the most commonly recovered causative organism in contact lens–related disease.[21,22] Currently, bacterial keratitis is mainly treated by the topical administration of antibiotics; however, the frequent emergence of antibiotic-resistant bacteria poses serious challenges for effective management.[23] Development of alternative treatment depends on discoveries of new molecular mechanisms and therapeutic targets. In this regard, we showed that miR-183C is expressed in innate immune cells, including macrophages (Mϕ) and polymorphonuclear leukocytes (PMNs), and modulates their phagocytosis and intracellular bacterial killing capacity, as well as their inflammatory response to bacterial infection by targeting Nox2 and DAP12.[10,24] Inactivation of miR-183C in mice resulted in decreased production of proinflammatory cytokines and reduced the severity of PA keratitis.[10,24] These data suggest that miR-183C is a potential therapeutic target for the treatment of PA keratitis, leading us to hypothesize that local knockdown of miR-183C in the cornea reduces PA keratitis through enhancing host innate immunity.

To test this hypothesis, we performed a prophylactic study in which subconjunctival injection and topical application of LNA-modified anti-miR-183C were used in a PA keratitis mouse model. Here, we provide evidence that local knockdown of miR-183C by anti-miR application prophylactically ameliorates PA keratitis.

Methods

Mice

All experiments and procedures involving animals and their care were reviewed and approved by the Wayne State University Institutional Animal Care and Use Committee and carried out in accordance with National Institute of Health and ARVO guidelines. The miR-183C$^{GT/+}$ mice are on a 129S2/BL/6-mixed background.[25] Young adult (8 weeks old), wild-type (WT) mice (miR-183C$^{+/+}$), derived from the miR-183C^{GT} colony, were used in the initial trial. To avoid variation of the genetic background, age, and sex, 8-week-old female C57BL/6 mice (000664; The Jackson Laboratory, Bar Harbor, ME, USA) were used for subsequent experiments regarding PA infection and prophylactic treatment. To study miRNA/target relationships, 12-week-old, male miR-183C knockout mice (miR-183C$^{GT/GT}$) and their age- and sex-matched WT controls were used to isolate total RNA from their trigeminal ganglia (TG) and corneas for gene expression analysis.

In Vitro Transfection of Anti-miR-183C in Raw264.7 Cells

LNA-modified anti-miR-183, anti-miR-96, and anti-miR-182 (LNA–anti-miR-183C), as well as negative control ORNs with scrambled sequences (NC ORNs) were purchased from QIAGEN (Hilden, Germany. YI04101800-DFA, YI04102572-DFA, YI04101243-DFA, and YI00199006-DFA). Also, 4×10^5 RAW264.7 Mϕ-like cells (a cell line derived from the mouse; American Type Culture Collection, Manassas, VA, USA) were plated in 48-well plates and transfected with LNA–anti-miR-183C (10 nM each) or NC ORNs (30 nM) using RNAiMax Lipofectamine (Thermo Fisher Scientific, Waltham, MA, USA) as described before.[26] All experiments were conducted with three replicate wells. Forty-eight hours after transfection, cells were harvested to prepare miRNA-proof total RNA for quantitative RT-PCR (RT-qPCR) analysis as described below.

Subconjunctival and Topical Application of LNA–Anti-miR-183C and PA Infection of the Cornea

Subconjunctival injection of 5 µL of LNA–anti-miR-183C or NC ORNs in sterile saline (8 mM each) was performed 1 day before PA infection, as described previously.[24,27,28] Briefly, mice were anesthetized with ethyl ether in a well-ventilated hood. The cornea of the left eye was scarified with a 25 5/8-gauge needle. Three 1-mm incisions were made to the corneal surface, which penetrated the epithelial layer, no deeper than the superficial stroma. Then, 5.0×10^6 colony forming units (CFUs) of PA (strain 19660; American Type Culture Collection) in a 5-µL volume was topically delivered. Six hours after PA infection and once daily thereafter, 5 µL of LNA–anti-miR-183C or NC ORNs in sterile saline (4 µM/each) was topically applied to the infected cornea. Corneal disease was graded at 1, 3, and 5 dpi using an established scale[28]: 0, clear or slight opacity, partially or fully covering the pupil; +1, slight opacity, covering the anterior segment; +2, dense opacity, partially or fully covering the pupil; +3, dense opacity, covering the entire anterior segment; and +4, corneal perforation. Photography with a slit lamp was used to illustrate disease at 5 dpi. The corneas were harvested for various assays at 1 and/or 5 dpi as detailed below.

To test the effect of anti-miR-183C alone on corneal nerves, anti-miR-183C or NC ORNs were subconjunctivally injected and topically applied to the cornea of C57BL/6 mice using the same prophylactic regimen but without PA infection. After 5 days of topical application, immunofluorescence (IF) in flatmounted corneas with anti-β-tubulin III antibody was done and corneal nerve density was determined.

To trace LNA–anti-miR-183C in the cornea, fluorescein amidite (FAM)-labeled LNA–anti-miR-183C (QIAGEN miRCURY LNA miRNA Power Inhibitors YI04101800-DDC, YI04102572-DDC, and YI04101243-DDC) or QIAGEN NC ORNs (YI00199006-DDC) were subconjunctivally injected and/or topically applied and tested by flow cytometry analysis or laser scanning confocal microscopy (see details below).

RNA Preparation and RT-PCR

Total RNA was prepared using the Life Technologies mirVana miRNA Isolation Kit (Thermo Fisher Scientific) or the QIAGEN RNeasy kit for miRNA or mRNA studies, as described previously.[29–31] RT-qPCR for miRNAs was performed using Applied Biosystems TaqMan miRNA primers (Thermo Fisher Scientific) and a RT-PCR kit with snRNA U6 as an endogenous control as described before.[30,31] RT-qPCR of protein-coding genes was performed using the QIAGEN QuantiFast SYBR Green RT-PCR Kit and QuantiTect Primer Assays with 18S rRNA as endogenous controls.[25,30,31]

ELISA

Protein levels for IL-1β, monocyte chemoattractant protein 1 (MCP1), and macrophage inflammatory protein 2 (MIP-2) were tested using ELISA kits (R&D Systems, Minneapolis, MN, USA) as described before.[10,24] Briefly, corneas were homogenized in 1 mL of PBS with 0.1% Tween 20 and

protease inhibitors (Sigma-Aldrich, St. Louis, MO, USA). An aliquot of each supernatant was assayed in duplicate per the manufacturer's instructions. Sensitivities of the ELISA assays were <2.31 pg/mL for IL-1β, <2 pg/mL for MCP1, and <1.5 pg/mL for MIP-2.

Quantitation of PMNs

A myeloperoxidase (MPO) assay was performed as described before.[24] Briefly, corneas were harvested, homogenized in 1 mL potassium phosphate buffer (50 mM, pH 6.0) containing 0.5% hexadecyltrimethylammonium bromide (Sigma-Aldrich). After four freeze/thaw cycles, 100 µL supernatant was added to 2.9 mL *o*-dianisidine dihydrochloride substrate buffer (16.7 mg/mL) with 0.0005% hydrogen peroxide. The change in absorbance at 460 nm was read every 30 seconds for 5 minutes on a Helios Alpha Spectrophotometer (Thermo Fisher Scientific). Units of MPO per cornea were calculated; 1 unit of MPO activity is equivalent to $\sim 2 \times 10^5$ PMNs.[32]

Quantitation of Viable Bacteria

Bacteria were quantitated as described before.[24] Briefly, each cornea was homogenized in 1.0 mL sterile saline containing 0.25% BSA. Then, 0.1 mL of the corneal homogenate was serially diluted (1:10) in the same solution, and selected dilutions were plated in triplicate on *Pseudomonas* isolation agar (BD Biosciences, Franklin Lakes, NJ, USA). Plates were incubated overnight at 37°C, and the number of colonies was counted. Results are reported as $\log_{10}$ number of CFUs per cornea ± SEM.

Immunofluorescence

Rat Anti-Mouse F4/80 (MCA497R, clone CI:A3-1, 1/400 dilution; Bio-Rad Laboratories, Hercules, CA, USA) and Mouse Anti-β-Tubulin III (801201, 1/600 dilution; BioLegend, San Diego, CA, USA) antibodies were used. Goat Anti-Rat IgG (A11081; 1/1000 dilution) and Goat Anti-Mouse IgG (A-11003, 1/1000 dilution) were purchased from Thermo Fisher Scientific.

Flatmount cornea and corneal stroma preparation and IF were performed as described previously.[33] Briefly, mice were euthanized, the eyes were enucleated, and the cornea anterior to the limbus was carefully dissected out. For whole-cornea flatmount microscopy, the cornea was transferred to 1% paraformaldehyde (PFA) in 0.1-M phosphate buffer, pH 7.4, for 1 hour at 4°C. After washing, the cornea was flattened with four to six evenly spaced cuts from the periphery toward the center and mounted in VECTASHIELD media with 4′,6-diamidino-2-phenylindole (DAPI; Vector Laboratories, Burlingame, CA, USA) on Fisherbrand Superfrost Plus slides (Thermo Fisher Scientific).

For IF of the whole cornea, the cornea was fixed in 1% PFA and then incubated in a blocking buffer with 5% normal goat serum (NGS; Vector Laboratories) in PBS+ (PBS plus 2-mM $MgCl_2$) for 30 minutes at room temperature (RT) and then permeabilized with 0.1% Triton X-100 in the blocking buffer for 30 minutes at RT. Subsequently, corneal tissues were incubated with primary antibodies in the blocking buffer for 72 hours at 4°C. After washes in PBS+, the corneal tissues were incubated with secondary antibodies for 24 hours at 4°C.

For IF of the corneal stromal layer, before fixation the cornea was incubated in 20-mM EDTA in PBS at 37°C for 40 minutes. Subsequently, after the epithelial layer was peeled away, the stroma was fixed in 1% PFA and then incubated in a blocking buffer with 5% NGS in PBS+ for 30 minutes at RT and then permeabilized with 0.1% Triton X-100 in the blocking buffer for 30 minutes at RT. Subsequently, corneal tissues were incubated with primary antibodies in the blocking buffer overnight at 4°C. After washes in PBS+, the corneal tissues were incubated with secondary antibodies for 2 hours at RT, and the corneal tissues were flattened and mounted on slides. All slides were studied and imaged using a TCS SP8 laser scanning confocal microscope (Leica Microsystems, Wetzlar, Germany). Negative controls were treated similarly but with the omission of primary antibody.

Quantification of Corneal Nerve Density

Corneal nerve density was determined as described before with minor modifications.[34,35] Briefly, Z-stack images were acquired from the central and pericentral regions of the cornea ($\sim$500 µm^2/area) with a comparable thickness ($\sim$50 µm) using the TCS SP8 laser confocal microscope. The images were collapsed to two dimensions and converted to a binary image using ImageJ 1.52p (National Institutes of Health, Bethesda, MD, USA). The nerve area was obtained using the histogram tool. Three corneas were obtained from three mice for each condition.

Flow Cytometry Analysis

A similar protocol as described before[33] was followed with modifications. Briefly, corneas anterior to the limbus were excised, pooled, and incubated in Hank's Balanced Salt Solution with 0.2% collagenase A and 0.5 mg/mL DNase I (Sigma-Aldrich) for 75 minutes at 37°C. Corneas were triturated to a single-cell suspension and then filtered through a 70-µm filter (Miltenyi Biotec, Bergisch Gladbach, Germany). Cells were resuspended in fluorescence-activated cell sorting (FACS) buffer and then incubated with Fixable Viability Dye eFluor 450 (Thermo Fisher Scientific) for 30 minutes on ice. After washing, the cells were incubated with FACS buffer containing 20 µg of Fc blocking antibody (purified anti-mouse CD16/32, clone 93; Thermo Fisher Scientific) and anti-mouse CD16.2 antibody (FcγRIV; clone 9E9; BioLegend) on ice for 10 minutes. Subsequently, cells were stained with an antibody cocktail for 30 minutes. The antibody cocktail included APC/Fire 750 CD45 antibody (clone 30-F11; BioLegend), BUV395 CD11b antibody (clone M1/70; BD Biosciences), PE-F4/80 antibody (clone BM8; Thermo Fisher Scientific), PE/Dazzle 594 CD11c antibody (clone 223H7; BioLegend), PerCP-eFluor 710-Ly6G (Gr-1; clone 1A8-Ly6g; eBioscience), Brilliant Violet 785 anti-mouse Ly-6C antibody (clone HK1.4; BioLegend), APC Langerin antibody (CD207, clone 4C7; BioLegend), and Alexa Fluor 700 anti-Mouse I-A/I-E Antibody (clone M5/114.15.2; Thermo Fisher Scientific) in BD Horizon Brilliant Stain Buffer (BD Biosciences). After washing, cell profiles were analyzed on a SY3200 Cell Sorter (Sony Corporation, Tokyo, Japan) at the Microscopy, Imaging and Cytometry Resources Core, Wayne State University. Invitrogen UltraComp eBeads Compensation Beads (Thermo Fisher Scientific) were used to optimize fluorescence compensation settings for multicolor flow cytometry. Data analysis was performed using FlowJo v10 software.

Investigative Ophthalmology & Visual Science

Statistical Analysis

Statistical analysis was performed as described before.[24,33] Briefly, the difference in clinical scores between groups was tested by the Mann–Whitney *U* test. One-way ANOVA with Bonferroni test (Prism; GraphPad, San Diego, CA, USA) was used to analyze RT-qPCR data for cytokine/chemokine mRNA levels. Adjusted $P < 0.05$ was considered significant. An unpaired, two-tailed Student's *t*-test was used to determine the significance of RT-qPCR of miRNAs, ELISA, MPO, and plate count data. Each experiment was repeated at least once to ensure reproducibility. Data from a representative experiment are shown. Quantitative data are expressed as the mean ± SEM.

Results

LNA–Anti-miR-183C Downregulates the Expression of miR-183C In Vitro and In Vivo

To test whether anti-miR-183C efficiently downregulates the expression of miR-183C, we first performed an in vitro transfection experiment in Mϕ-like Raw264.7 cells. Forty-eight hours after transfection of LNA–anti-miR-183C (10 nM/each), the expression of all three members of miR-183C was significantly downregulated (Fig. 1A). To test whether anti-miR-183C knocks down the expression of miR-183C in PA-infected cornea in vivo, we subconjunctivally injected miR-183C WT mice with LNA–anti-miR-183C (5 µL and 8 µM in sterile saline each) 1 day before infection and then topically applied the anti-miRs to the infected cornea (5 µL and 4 µM in sterile saline each) once daily after infection. LNA–NC ORNs were used in parallel as a negative control. At 5 dpi, we harvested the corneal RNA for RT-qPCR analysis. Our data showed that the application of LNA–anti-miR-183C resulted in significantly decreased expression of all members of miR-183C, suggesting that this regimen can be used to test the effect of local knockdown of miR-183C in PA keratitis.

Local Knockdown of miR-183C Resulted in Decreased Severity of PA Keratitis

To test whether local knockdown of miR-183C in the cornea has any beneficial effect on PA keratitis, we followed the same schedule of subconjunctival and topical application of LNA–anti-miRs and PA infection in 8-week-old female C57BL/6 inbred mice that are susceptible to PA infection.[36] Our data showed that local application of LNA–anti-miR-183C consistently resulted in significantly decreased severity of PA keratitis at 3 and 5 dpi (Fig. 2), suggesting that local knockdown of miR-183C in the cornea has a beneficial effect and decreases disease.

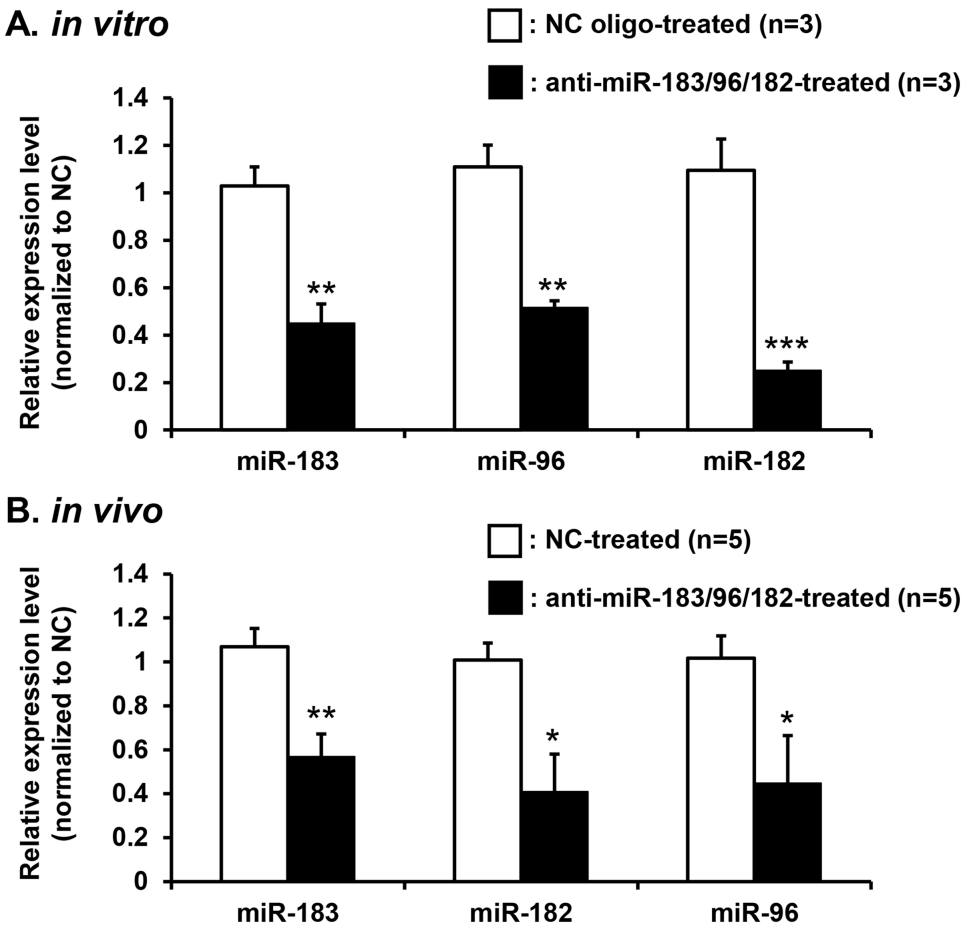

Figure 1. Anti-miR-183/96/182 downregulates the expression of miR-183/96/182 in vitro (A) and in vivo (B). RT-qPCR analysis of miR-183/96/182 in Raw264.7 cells 48 hours after the transfection of LNA–anti-miR-183/96/182 (A) and in PA-infected mouse corneas subjected to subconjunctival injection and topical application of anti-miR-183/96/182 (B). *$P < 0.05$; **$P < 0.01$; ***$P < 0.001$.

Investigative Ophthalmology & Visual Science

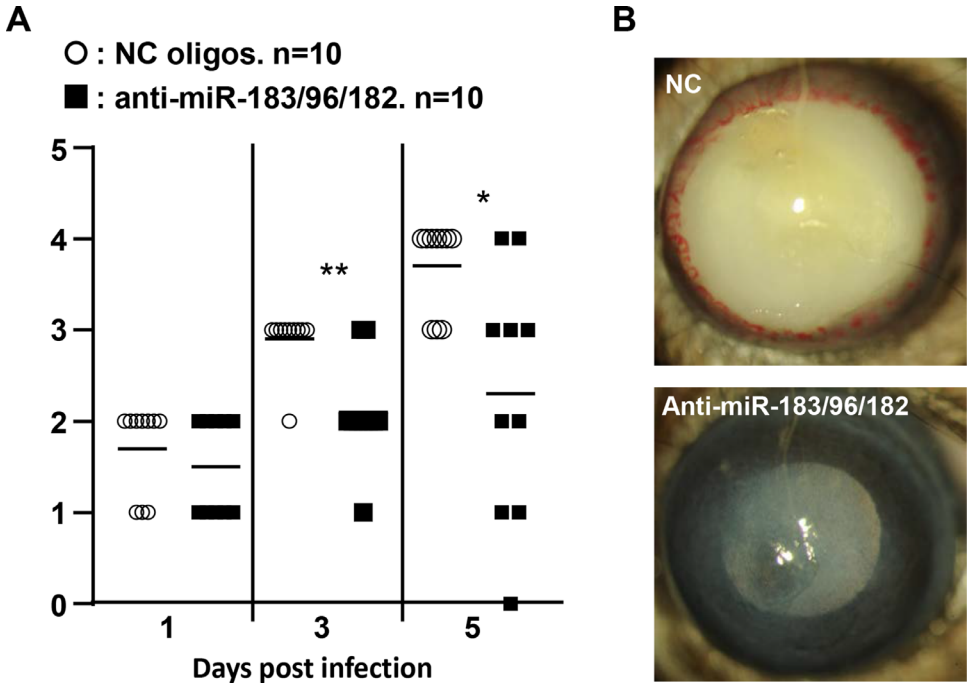

Figure 2. Local application of LNA–anti-miR-183/96/182 resulted in a decreased severity of PA keratitis. (A) Clinical scores. *Horizontal bars* represent the mean values. (B) Examples of slit-lamp photography of eyes of NC and anti-miR-183/96/182–treated animals at 5 dpi. $^{*}P < 0.05$; $^{**}P < 0.01$.

Local Knockdown of miR-183C Led to Changes in the Expression of Proinflammatory Cytokine/Chemokine IL-1β in Response to PA Infection

To test the inflammatory response in the cornea after PA infection, we harvested total corneal RNA at 5 dpi and performed RT-qPCR to test for proinflammatory cytokines/chemokines, IL-1β, Cxcl2 (MIP2), and Ccl2 (MCP1). Our results showed no significant difference in the levels of these genes at the mRNA level between the anti-miR-183C–treated and NC ORN–treated animals (Fig. 3A). To further investigate the inflammatory response of the cornea to PA infection at the protein level, we performed ELISA assays on total corneal protein lysate at 1 and 5 dpi. IL-1β protein was significantly upregulated at 1 dpi but significantly decreased at 5 dpi in the anti-miR-183C–treated versus NC ORN–treated corneas (Fig. 3B). However, MIP2 and MCP1 showed no significant difference between the anti-miR–treated and the NC ORN–treated corneas at the protein level (Fig. 3B).

Anti-miR-183C Treatment Resulted in Decreased PMN at 5 Days Post-Infection

The innate immune system plays a major role in the corneal response to PA infection.[21,28,37–41] Mϕ and PMN are the predominant infiltrating cells. PMNs, along with Mϕ, are recruited to the cornea to engulf bacteria while producing large amounts of reactive oxygen species (ROS) and reactive nitrogen species (RNS), which kill engulfed bacteria and contribute to bacterial clearance.[21,37–41] However, persistence of PMNs often occurs and is associated with increased tissue damage and corneal perforation.[28,37–41] To test the effect of local knockdown of miR-183C in the cornea on PMN infiltration, we performed an MPO assay to enumerate the cells.[32] Our results showed that, although not different between groups at 1 dpi, the number of PMNs in the LNA–anti-miR-183C–treated eyes was significantly decreased at 5 dpi when compared with NC ORN–treated control eyes (Fig. 4).

Local Knockdown of miR-183C Resulted in Decreased Bacterial Load at Both 1 and 5 dpi

Resolution of PA keratitis depends on clearance of the bacteria in addition to healing of the corneal tissues. To test the effect of anti-miR-183C on the clearance of PA, we performed plate counts of the residual bacteria in cornea at 1 and 5 dpi. We found that the number of residual bacteria was significantly decreased in the LNA–anti-miR-183C–treated versus NC ORN–treated corneas at both 1 and 5 dpi (Fig. 5), suggesting that local knockdown of miR-183C resulted in enhanced bacterial clearance.

Anti-miR-183C Transfection of Mϕ and Dendritic Cells Increased Their Expression of MHCII

To track the anti-miRs in the cornea, we employed FAM-labeled LNA–anti-miR-183C or NC ORNs for subconjunctival injection 1 day before and topical applications once daily after PA infection. At 5 dpi, we harvested the cornea for flow-cytometry analysis. Our results showed that the percentages of FAM^{+} cells in total corneal cells, or in Mϕ, dendritic cells (DCs), PMN, and $CD45^{-}$ cells, are similar between LNA–anti-miR-183C– and NC ORN–treated corneas (Table), suggesting that the sequences of the LNA-labeled ORNs, either the LNA–anti-miRs or NC ORNs, have no influence on the transfection

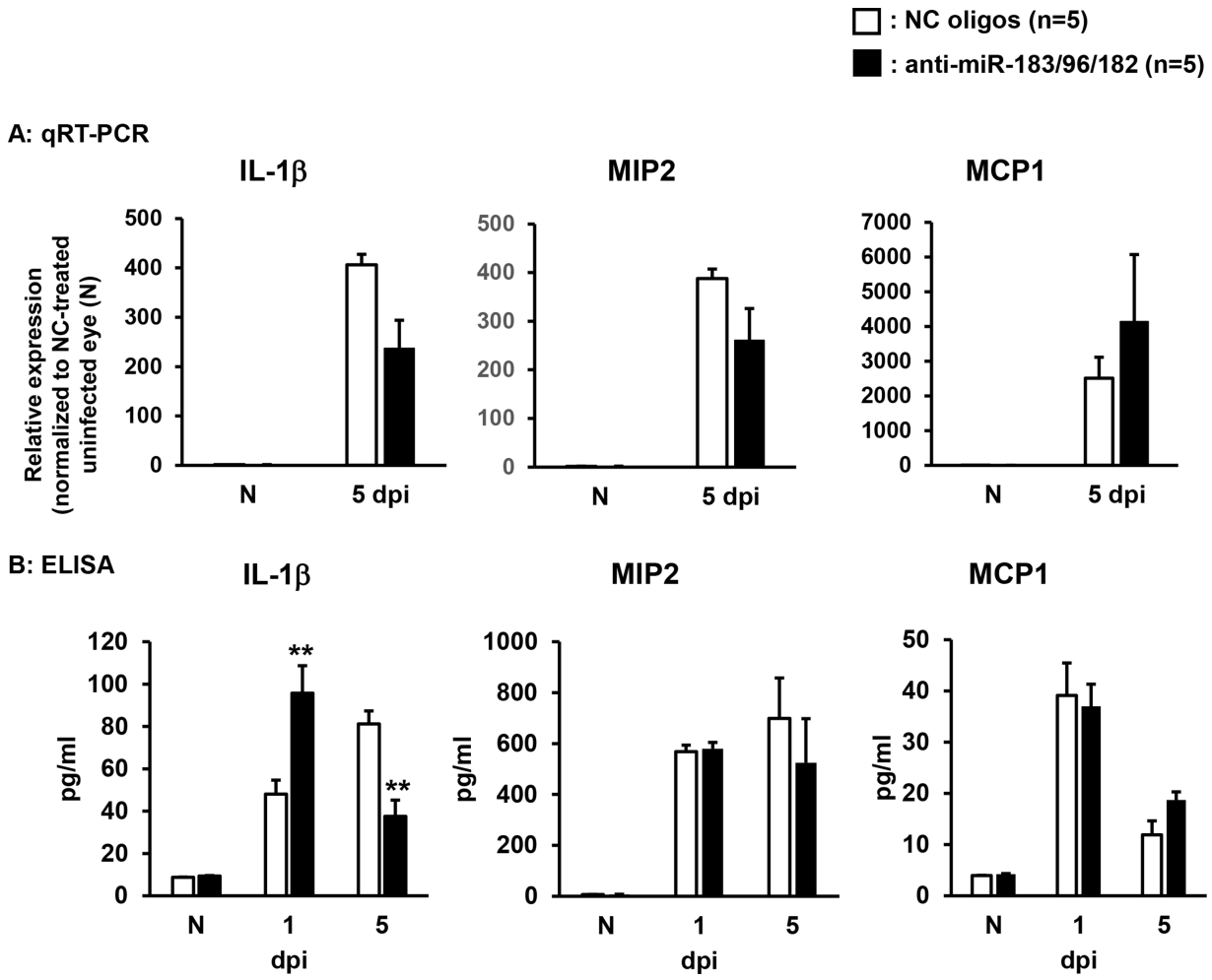

Figure 3. Knockdown of miR-183/96/182 in the cornea resulted in changes of the production of proinflammatory cytokine/chemokine production. (A) RT-qPCR. (B) ELISA assays (n = 5/group). $^{**}P < 0.01$.

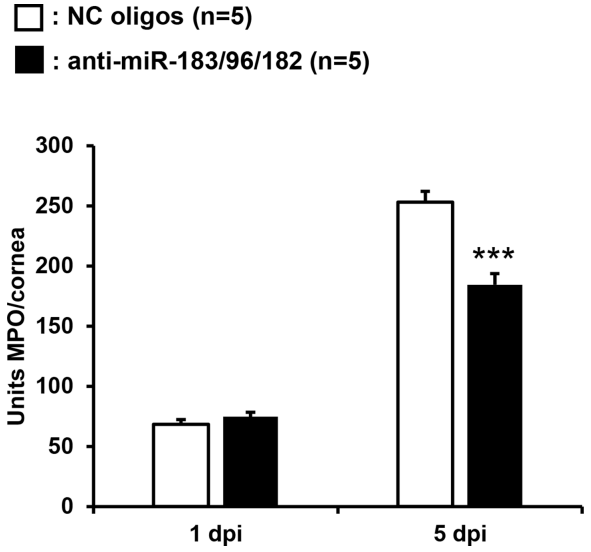

Figure 4. Knockdown of miR-183/96/182 in the cornea resulted in significantly decreased MPO levels in the cornea at 5 dpi of PA infection (n = 5/group). $^{***}P < 0.001$.

efficiency in different cell types of the cornea in vivo. Therefore, we merged the data from both LNA–anti-miR-183C– and NC ORN–treated corneas to reveal an overall in vivo transfection efficiency in different cell types by the LNA-modified ORNs. The combined data demonstrated that, although only 4.70% (±0.65%), 2.04% (±0.38%), and 3.30 (±0.41%) of total corneal cells, PMNs, and CD45$^-$ non-hematopoietic cells, respectively, in the cornea are FAM$^+$, 22.16% (±4.20%) of Mϕ and 32.38% (±6.08%) of DCs are FAM$^+$ (Table, Fig. 6A), which is consistent with their phagocytotic functions.[42–45]

Although there were no significant differences in the number of CD45$^+$ leukocytes, Mϕ (CD45$^+$CD11b$^+$F4/80$^+$) and DCs (CD45$^+$CD11b$^+$Ly6G$^+$) in the cornea between LNA–anti-miR-183C– and NC ORN–treated corneas (data not shown), the percentage of MHCII$^+$ (I-A/I-E$^+$) cells among Mϕ and DCs were significantly increased in anti-miR-treated corneas (3.04% ± 0.74% and 8.48% ± 1.36%, respectively), when compared with NC ORN–treated corneas (0.83% ± 0.18% and 3.36% ± 1.03%, respectively) (Figs. 6B, 6C), suggesting that transfection of anti-miR-183C resulted in increased maturation/activation of Mϕ and DCs.[46–48] Additional anti-miR tracing experiments on scarified cornea without bacterial infection showed that topically applied LNA–anti-miRs could be detected as early as 6 hours after the application of the anti-miRs and remained detectable by

Investigative Ophthalmology & Visual Science

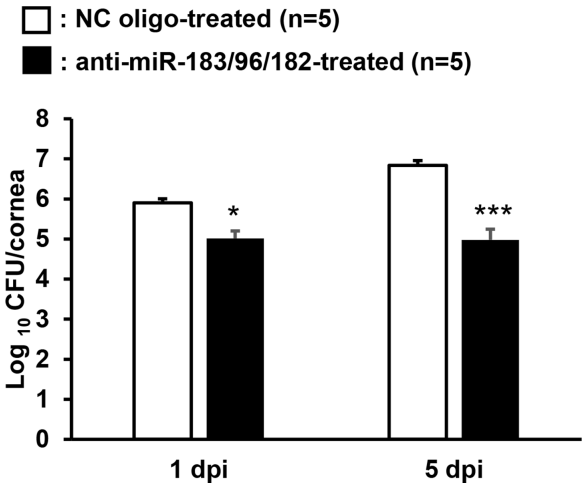

Figure 5. Knockdown of miR-183/96/182 in the cornea resulted in significantly decreased bacterial load in the cornea at both 1 and 5 dpi of PA infection ($n = 5$/group). *$P < 0.05$; ***$P < 0.001$.

3 days post-application (dpa) in the cornea (Fig. 7A), with most of the anti-miRs appearing to stay in the vicinity of the scarified area (Fig. 7A). Transfection of Mϕ was further confirmed by IF at 3 dpa (Fig. 7B).

Knockdown of miR-183C in the Cornea Results in Transient and Reversible Corneal Nerve Density Reduction

To test the effect of anti-miR-183C alone on corneal nerves, anti-miR-183C or ORN were subconjunctivally injected and topically applied to the cornea of C57BL/6 mice using the same prophylactic regimen but without PA infection. After 5 days of topical application, IF using β-III tubulin antibody was done to quantify the corneal nerve density (Fig. 8). Results showed that anti-miR-183C versus NC ORN treatment decreased nerve density (Figs. 8D–8F vs. Figs. 8A–8C). This effect is most prominent in the central area of the subbasal plexus (Figs. 8E vs. Figs. 8B and 8J), similar to what is seen in uninfected miR-183C knockout versus WT control mice.[24] These data further support that miR-183C regulates corneal sensory innervation and suggest that corneal nerve reduction may contribute to the protective effect of anti-miR treatment.

To test whether anti-miR-183C–induced reduction of corneal nerves causes permanent changes to corneal innervation, after the last topical application another group of anti-miR–treated mice was held for another week without any treatment. Their corneal nerve density was fully recovered (Figs. 8G–8J), suggesting that anti-miR-183C–induced corneal nerve density reduction is a transient effect and reversible after withdrawal of anti-miR application.

Target prediction using TargetScan (TargetScan.org)[49–53] and miRWalk (mirwalk.umm.uni-heidelberg.de/) algorithms[54] indicated that neuropilin 1 (Nrp1),[55] a negative regulator of corneal nerve growth into the cornea during development[56,57] and of corneal nerve preservation in dry eye disease[58] and regeneration during epithelial wound healing,[59,60] is a predicted target of miR-183 and miR-182 (Fig. 8K, left). Consistently, Nrp1 is upregulated in the TG, where cell bodies of corneal sensory nerves reside, of naïve miR-183C knockout mice (Fig. 8K, right), suggesting that miR-183C targets Nrp1 in TG neurons, which potentially could contribute to the anti-miR-183C–induced reduction of corneal nerve density.

Discussion

Previously, we determined that the conserved miR-183C cluster is expressed in innate immune cells (e.g., Mϕ, PMNs) in both mouse and human[24] and imposes cell-type specific regulation of their functions.[10,24,33] Knockdown or inactivation of miR-183C in mouse peripheral Mϕ and PMN enhances their phagocytotic and intracellular bacterial killing capacity,[24] which is mediated, at least in part, by increased production of ROS and RNS.[10] Downregulation of miR-183C in peripheral Mϕ in mouse results in reduced production of proinflammatory cytokines/chemokines, including IL-1β, MIP2, and MCP1, in response to PA and/or its outer membrane component, lipopolysaccharide.[10] The miR-183C knockout mice showed an overall reduced expression of proinflammatory cytokines/chemokines in the cornea and deceased severity of PA keratitis.[24] Therefore, we hypothesized that downregulation of miR-183C in the cornea may have a beneficial effect on ameliorating PA keratitis.

Here, we show that knockdown of miR-183C by subconjunctival injection 1 day before and topical application of LNA–anti-miR-183C once daily after PA infection in mice resulted in initial elevated IL-1β protein levels at 1 dpi, decreased IL-1β protein levels and number of PMNs at 5 dpi, reduced bacterial load in the cornea at both 1 and 5 dpi, and, ultimately, decreased severity of disease. These results suggest that local knockdown of miR-183C protects the cornea from severe PA keratitis, providing the first direct evidence that miR-183C is a potential therapeutic target for its treatment.

Further supporting this hypothesis, our anti-miR tracing experiments showed that single doses of topically applied LNA–anti-miRs lasted for at least 3 days and transfected Mϕ in the corneal tissue. Flow cytometry confirmed that Mϕ and DCs in the cornea showed the highest rates of transfection by LNA–anti-miRs in PA infected cornea, consistent with their phagocytic functions.[42–45] Moreover, knockdown of miR-183C resulted in an increased percentage of MHCII$^+$ Mϕ and DCs in PA-infected cornea,

Table. Percentage of FAM$^+$ Cells in Various Cell Populations of the Cornea

	Average ± SEM				
	Total Live Cells	**Mϕ**	**DCs**	**PMNs**	**CD45$^-$ Cells**
NC oligo-treated ($n = 3$)	4.26 ± 0.27	19.24 ± 7.17	32.89 ± 11.83	1.77 ± 0.11	3.11 ± 0.29
Anti-miR-treated ($n = 3$)	5.13 ± 1.37	25.07 ± 5.33	31.87 ± 6.67	2.31 ± 0.80	3.49 ± 0.86
Combined ($n = 6$)	4.70 ± 0.65	22.16 ± 4.20	32.38 ± 6.08	2.04 ± 0.38	3.30 ± 0.41

Investigative Ophthalmology & Visual Science

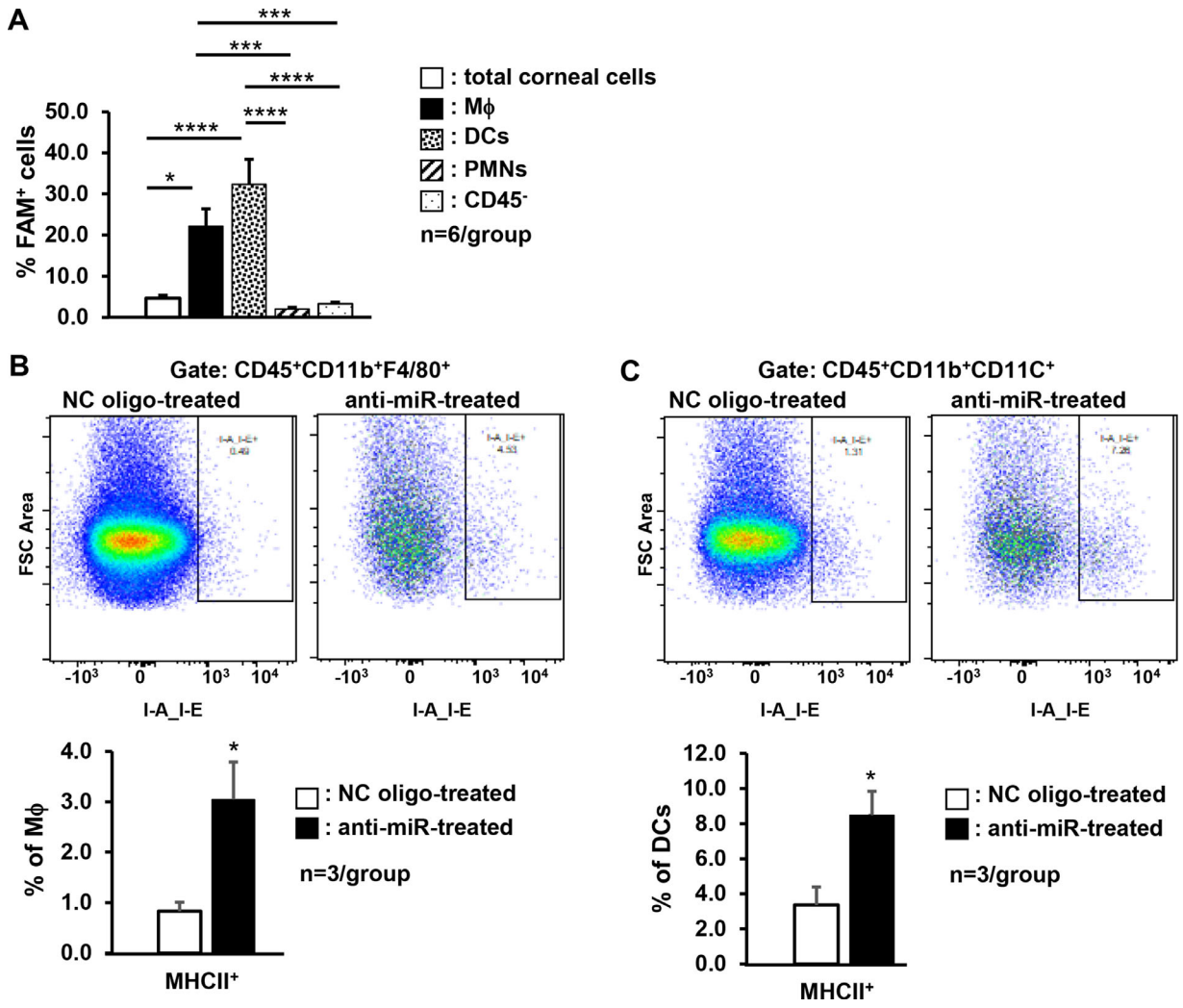

Figure 6. Local knockdown of miR-183/96/182 resulted in significantly increased expression of MHCII in Mϕ and DCs in the PA-infected corneas. Flow cytometry analysis on PA-infected, FAM-labeled anti-miR-183/96/182– and NC ORN–treated corneal cells at 5 dpi. (A) Percentage of FAM^+ cells in total corneal cells, Mϕ ($CD45^+CD11b^+F4/80^+$), DCs ($CD45^+CD11b^+CD11C^+$), and non-hematopoietic cells in the cornea ($CD45^-$) in all animals ($n = 6$). (B, C) Comparison of percentage of $MHCII^+$ ($I\text{-}A/I\text{-}E^+$) cells in Mϕ (B) and DCs (C). $^*P < 0.05$, $^{***}P < 0.001$; $^{****}P < 0.0001$.

suggesting enhanced activation/maturation of these innate immune cells.[46–48] Because innate immune cells play a major role in the corneal responses to PA infection,[21,28,37–41] these data provide the first clues to the underlying mechanism of the therapeutic effects of anti-miR-183C, suggesting that downregulation of miR-183C in the Mϕ and DCs plays a role in the overall effect of anti-miR-183C on PA keratitis.

Innate immune cells play a pivotal role in the pathogenesis of PA keratitis,[21,28,37–41] with PMN representing the predominant class of infiltrating cells. Along with Mϕ, PMNs are recruited to engulf bacteria and produce large amounts of bactericidal ROS and RNS, responsible for bacterial clearance.[21,37–41] However, persistence of PMN is associated with increased tissue damage and perforation.[28,37–41] Our data showed that, although the anti-miR-183C–treated PA-infected cornea had similar PMN numbers at 1 dpi, which decreased at 5 dpi, the number of residual bacteria in the cornea was significantly decreased at both 1 and 5 dpi when compared with the NC ORN–treated corneas. One of the possible explanations of this observation is that, as we showed previously,[10,24] knockdown of miR-183C in PMNs and Mϕ enhanced their phagocytosis and bacterial killing capacity or efficiency, resulting in an overall decreased number of residual bacteria with fewer PMNs. The timely decreased number of PMNs at 5 dpi may have contributed to reduced collateral damage to corneal tissue and, therefore, decreased severity of PA keratitis in the anti-miR–treated cornea. However, the decreased numbers of residual bacteria at 1 and 5 dpi are unlikely to be fully explained by enhanced phagocytosis and bacterial killing capacity of PMNs and Mϕ. More studies on the dynamics, cytokine production, and bactericidal functions of corneal resident and infiltrating Mϕ and PMNs in the anti-miR–treated corneas in the context of PA infection are required to further confirm these hypotheses.

Originally, miR-183C was identified as a sensory organ–enriched miRNA cluster.[30] It is highly expressed in all sensory neurons.[25,30,61,62] We and others have shown that miR-183C is required for normal vision,[25] hearing and balance,[25,63–66] olfaction,[64] touch, and mechanical and

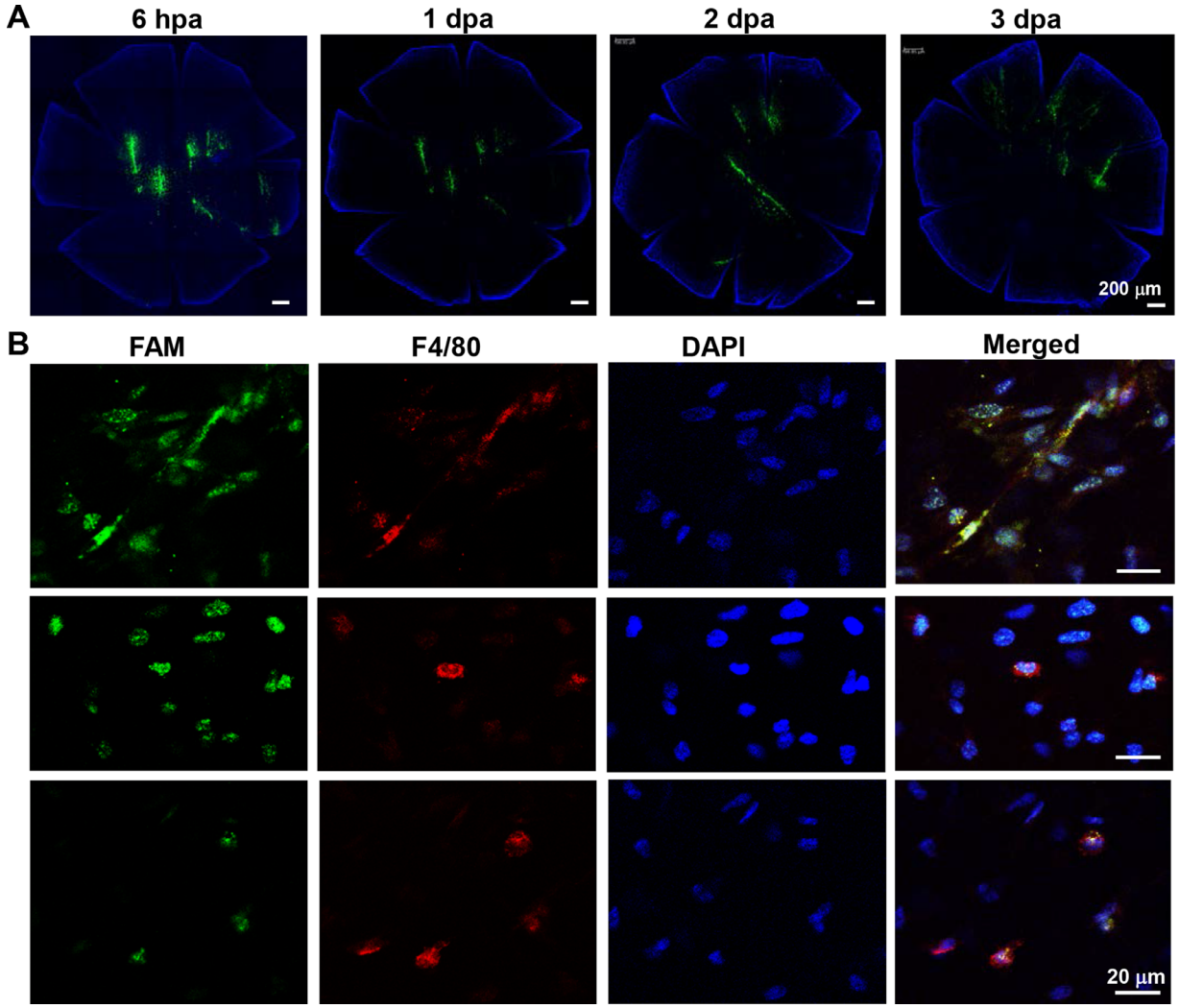

Figure 7. Topical application of FAM-labeled LNA–anti-miR-183 leads to transfection of Mϕ in the cornea. Five microliters of anti-miR-183 in sterile saline (4 mM each) was topically applied to scarified corneas, with the deepest wounds penetrating the epithelial basal lamina and into the superficial corneal stroma. The corneas were harvested at 6 hours post-application (hpa) and 1, 2, and 3 days post-application (dpa) for flatmount confocal microscopy (A) and IF with anti-F4/80 antibody (B). All samples in (B) are from 3 dpa.

neuropathic pain.[67] We demonstrated that miR-183C plays an important role in neuroimmune interaction in the cornea.[24] Its inactivation in mice causes decreased corneal nerve density, reduced expression of TRPV1, disruption of the normal whorl-like pattern of the subbasal nerve plexus, and decreased expression of proinflammatory neuropeptides in the cornea, including *Tac1*, the precursor gene for substance P (SP),[24] during disease resolution. SP is a chemoattractant and anti-apoptotic neuropeptide that enhances PMN infiltration and persistence in the cornea, the latter contributing to tissue damage and perforation.[28,37–41] Decreased neuropeptide expression, including SP, in the cornea of miR-183C knockout mice contributes to the decreased production of proinflammatory cytokines/chemokines and reduced severity of PA keratitis.[24] Consistent with these observations in the miR-183C knockout mice,[24] here we have shown that the application of anti-miR-183C to the cornea results in a transient and reversible reduction of corneal nerve density, with the whorl center of the subbasal nerve plexus being most affected. This may contribute to a decreased level of proinflammatory neuropeptide and neuroimmune/inflammatory responses in the cornea at a later stage of PA keratitis, similar to what was reported in miR-183C knockout mice.[24] The latter hypothesis is consistent with our observation of decreased IL-1β, reduced number of PMNs, and decreased severity of PA keratitis in anti-miR-183C versus NC ORN–treated mice. In the current study, to keep the uniformity of experimental condition, we used female C57BL/6 mice in the PA infection/prophylactic anti-miR treatment experiments. However, we are aware that, with new technological advances in science, sex-dependent differences have been reported in corneal nerves,[68] tissue resident immune cells, and innate immunity.[69–79] Therefore, we do not exclude the possibility that sex-dependent differences in the corneal response to PA infection upon anti-miR-183C treatment may exist. We will conduct such experiments in both male and females, separately, in future work.

With regard to potential mechanisms underlying anti-miR-183C–induced transient/reversible reduction of corneal nerve density, Nrp1 is a receptor for axon guidance molecules, such as semaphorin 3A (Sema3A).[55,56,80–85] Sema3A/Nrp1 interaction mediates repulsive or inhibitory

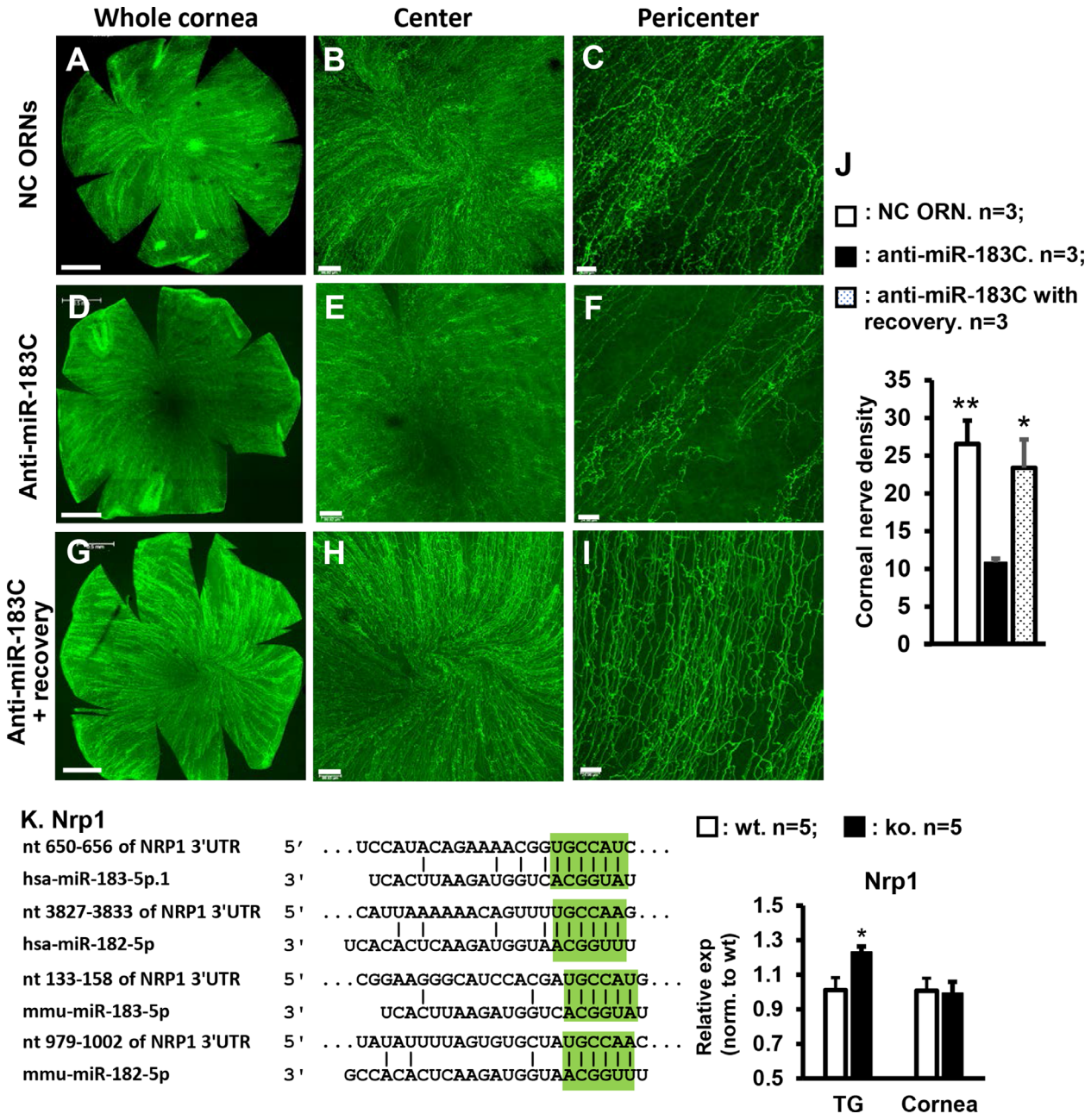

Figure 8. Anti-miR-183C treatment results in transient and reversible reduction of corneal nerve density. Compressed confocal microscopy images of β-III tubulin IF of flatmount corneas treated with NC ORNs (A–C), anti-miR-183C (D–F), or anti-miR-183C with 1-week recovery (G–I). *Scale bars*: 500 mm (A, D, G); 100 mm (B, E, H); and 25 mm (C, F, I). (J) Quantification of nerve density in the central area of the cornea (n = 3/condition; $^*P < 0.05$; $^{**}P < 0.01$) in comparison with anti-miR-183C–treated corneas. (K) miR-183C targets Nrp1. (*Left*) Sequence alignment of selected predicted target sites in human (hsa) and mouse (mmu) Nrp1 and miR-183 and miR-182. Residues in the *green box* are the seed sequences of the miRNAs, which are major determinants of target sites. nt, nucleotide; UTR, untranslated region. (*Right*) RT-qPCR with relative expression (exp) normalized (norm) to WT controls. Age, 12 weeks; sex, male; n = 5 per genotype. *Error bar*: SEM. $^*P < 0.05$.

guidance of corneal nerves during embryonic development[56,57,82,86] and in adult neurons.[81,84,85] Here, we showed that Nrp1 is a predicted target of miR-183C. Supporting this prediction, Nrp1 expression is increased in the TG of naïve miR-183C knockout mice, suggesting that miR-183C may regulate corneal growth and regression through its regulation of Nrp1 expression in TG neurons.

Collectively, our data suggest that, in addition to its regulation of innate immunity, miR-183C also modulates PA keratitis through regulation of corneal nerve growth and regression by targeting key molecules involved in corneal innervation and neuroimmune/inflammation interactions.

Conclusions

Our results show that local knockdown of miR-183C by the application of LNA–anti-miR-183C to the cornea has a prophylactic, protective effect against PA keratitis through its regulation of both innate immune/inflammatory response and corneal innervation and neuroimmune interaction.

Further studies are warranted to uncover the full potential and the underlying molecular mechanisms of anti-miR-183C in the treatment of microbial keratitis.

Acknowledgments

The authors thank Jessica Back and Eric VanBuren from the Microscopy, Imaging, and Cytometry Resources Core for their assistance in the flow cytometry and data analysis.

Supported by grants from the National Eye Institute, National Institutes of Health (R01 EY02605902 to SX; R01EY016058 and P30EY004068 to LDH), and by a Research to Prevent Blindness unrestricted grant to the Department of Ophthalmology, Visual and Anatomical Science, Wayne State University School of Medicine. The Microscopy, Imaging, and Cytometry Resources Core is supported by a Cancer Center Support Grant (P30 CA22453) from the National Cancer Institute, National Institutes of Health.

Disclosure: **S. McClellan**, None; **A. Pitchaikannu**, None; **R. Wright**, None; **D. Bessert**, None; **M. Iulianelli**, None; **L.D. Hazlett**, None; **S. Xu**, None

References

1. Ambros V. The functions of animal microRNAs. *Nature*. 2004;431:350–355.
2. Bartel DP. MicroRNAs: genomics, biogenesis, mechanism, and function. *Cell*. 2004;116:281–297.
3. Wightman B, Ha I, Ruvkun G. Posttranscriptional regulation of the heterochronic gene *lin-14* by *lin-4* mediates temporal pattern formation in *C. elegans*. *Cell*. 1993;75:855–862.
4. Lee RC, Feinbaum RL, Ambros V. The *C. elegans* heterochronic gene *lin-4* encodes small RNAs with antisense complementarity to *lin-14*. *Cell*. 1993;75:843–854.
5. Sontheimer EJ, Carthew RW. Silence from within: endogenous siRNAs and miRNAs. *Cell*. 2005;122:9–12.
6. Baek D, Villen J, Shin C, Camargo FD, Gygi SP, Bartel DP. The impact of microRNAs on protein output. *Nature*. 2008;455:64–71.
7. Selbach M, Schwanhausser B, Thierfelder N, Fang Z, Khanin R, Rajewsky N. Widespread changes in protein synthesis induced by microRNAs. *Nature*. 2008;455:58–63.
8. Chi SW, Zang JB, Mele A, Darnell RB. Argonaute HITS-CLIP decodes microRNA-mRNA interaction maps. *Nature*. 2009;460:479–486.
9. Nowakowski TJ, Rani N, Golkaram M, et al. Regulation of cell-type-specific transcriptomes by microRNA networks during human brain development. *Nat Neurosci*. 2018;21:1784–1792.
10. Muraleedharan CK, McClellan SA, Ekanayaka SA, et al. The miR-183/96/182 cluster regulates macrophage functions in response to *Pseudomonas aeruginosa*. *J Innate Immun*. 2019;11:347–358.
11. Boudreau RL, Jiang P, Gilmore BL, et al. Transcriptome-wide discovery of microRNA binding sites in human brain. *Neuron*. 2014;81:294–305.
12. Chang TC, Mendell JT. microRNAs in vertebrate physiology and human disease. *Annu Rev Genomics Hum Genet*. 2007;8:215–239.
13. Kloosterman WP, Plasterk RH. The diverse functions of microRNAs in animal development and disease. *Dev Cell*. 2006;11:441–450.
14. Alvarez-Garcia I, Miska EA. MicroRNA functions in animal development and human disease. *Development*. 2005;132:4653–4662.
15. Elmen J, Lindow M, Schutz S, et al. LNA-mediated microRNA silencing in non-human primates. *Nature*. 2008;452:896–899.
16. Krutzfeldt J, Rajewsky N, Braich R, et al. Silencing of microRNAs in vivo with 'antagomirs'. *Nature*. 2005;438:685–689.
17. Kota J, Chivukula RR, O'Donnell KA, et al. Therapeutic microRNA delivery suppresses tumorigenesis in a murine liver cancer model. *Cell*. 2009;137:1005–1017.
18. Henry JC, Azevedo-Pouly AC, Schmittgen TD. MicroRNA replacement therapy for cancer. *Pharm Res*. 2011;28:3030–3042.
19. Esau C, Davis S, Murray SF, et al. miR-122 regulation of lipid metabolism revealed by in vivo antisense targeting. *Cell Metab*. 2006;3:87–98.
20. Adams BD, Parsons C, Walker L, Zhang WC, Slack FJ. Targeting noncoding RNAs in disease. *J Clin Invest*. 2017;127:761–771.
21. Hazlett LD. Corneal response to *Pseudomonas aeruginosa* infection. *Prog Retin Eye Res*. 2004;23:1–30.
22. Stapleton F, Carnt N. Contact lens-related microbial keratitis: how have epidemiology and genetics helped us with pathogenesis and prophylaxis. *Eye (Lond)*. 2012;26:185–193.
23. Mesaros N, Nordmann P, Plesiat P, et al. *Pseudomonas aeruginosa*: resistance and therapeutic options at the turn of the new millennium. *Clin Microbiol Infect*. 2007;13:560–578.
24. Muraleedharan CK, McClellan SA, Barrett RP, et al. Inactivation of the miR-183/96/182 cluster decreases the severity of *Pseudomonas aeruginosa*-induced keratitis. *Invest Ophthalmol Vis Sci*. 2016;57:1506–1517.
25. Lumayag S, Haldin CE, Corbett NJ, et al. Inactivation of the microRNA-183/96/182 cluster results in syndromic retinal degeneration. *Proc Natl Acad Sci USA*. 2013;110:E507–E516.
26. Cowan C, Muraleedharan CK, O'Donnell JJ, 3rd, et al. microRNA-146 inhibits thrombin-induced NF-κB activation and subsequent inflammatory responses in human retinal endothelial cells. *Invest Ophthalmol Vis Sci*. 2014;55:4944–4951.
27. Huang X, Barrett RP, McClellan SA, Hazlett LD. Silencing Toll-like receptor-9 in *Pseudomonas aeruginosa* keratitis. *Invest Ophthalmol Vis Sci*. 2005;46:4209–4216.
28. Zhou Z, Barrett RP, McClellan SA, et al. Substance P delays apoptosis, enhancing keratitis after *Pseudomonas aeruginosa* infection. *Invest Ophthalmol Vis Sci*. 2008;49:4458–4467.
29. Li C, McClellan SA, Barrett R, Hazlett LD. Interleukin 17 regulates Mer tyrosine kinase-positive cells in *Pseudomonas aeruginosa* keratitis. *Invest Ophthalmol Vis Sci*. 2014;55:6886–6900.
30. Xu S, Witmer PD, Lumayag S, Kovacs B, Valle D. MicroRNA (miRNA) transcriptome of mouse retina and identification of a sensory organ-specific miRNA cluster. *J Biol Chem*. 2007;282:25053–25066.
31. Kovacs B, Lumayag S, Cowan C, Xu S. microRNAs in early diabetic retinopathy in streptozotocin-induced diabetic rats. *Invest Ophthalmol Vis Sci*. 2011;52:4402–4409.
32. Williams RN, Paterson CA, Eakins KE, Bhattacherjee P. Quantification of ocular inflammation: evaluation of polymorphonuclear leucocyte infiltration by measuring myeloperoxidase activity. *Curr Eye Res*. 1982;2:465–470.
33. Coku A, McClellan SA, Van Buren E, Back JB, Hazlett LD, Xu S. The miR-183/96/182 cluster regulates the functions of corneal resident macrophages. *Immunohorizons*. 2020;4:729–744.
34. Lin T, Quellier D, Lamb J, et al. *Pseudomonas aeruginosa*-induced nociceptor activation increases susceptibility to infection. *PLoS Pathog*. 2021;17:e1009557.

Investigative Ophthalmology & Visual Science

35. He J, Bazan HE. Neuroanatomy and neurochemistry of mouse cornea. *Invest Ophthalmol Vis Sci*. 2016;57:664–674.
36. Hazlett LD, McClellan S, Kwon B, Barrett R. Increased severity of *Pseudomonas aeruginosa* corneal infection in strains of mice designated as Th1 versus Th2 responsive. *Invest Ophthalmol Vis Sci*. 2000;41:805–810.
37. Kernacki KA, Barrett RP, Hobden JA, Hazlett LD. Macrophage inflammatory protein-2 is a mediator of polymorphonuclear neutrophil influx in ocular bacterial infection. *J Immunol*. 2000;164:1037–1045.
38. Kernacki KA, Barrett RP, McClellan S, Hazlett LD. MIP-1alpha regulates CD4+ T cell chemotaxis and indirectly enhances PMN persistence in *Pseudomonas aeruginosa* corneal infection. *J Leukoc Biol*. 2001;70:911–919.
39. Hazlett LD. Pathogenic mechanisms of *P. aeruginosa* keratitis: a review of the role of T cells, Langerhans cells, PMN, and cytokines. *DNA Cell Biol*. 2002;21:383–390.
40. Rudner XL, Kernacki KA, Barrett RP, Hazlett LD. Prolonged elevation of IL-1 in *Pseudomonas aeruginosa* ocular infection regulates macrophage-inflammatory protein-2 production, polymorphonuclear neutrophil persistence, and corneal perforation. *J Immunol*. 2000;164:6576–6582.
41. Kernacki KA, Barrett RP, McClellan SA, Hazlett LD. Aging and PMN response to *P. aeruginosa* infection. *Invest Ophthalmol Vis Sci*. 2000;41:3019–3025.
42. Guilliams M, Ginhoux F, Jakubzick C, et al. Dendritic cells, monocytes and macrophages: a unified nomenclature based on ontogeny. *Nat Rev Immunol*. 2014;14:571–578.
43. Reynolds G, Haniffa M. Human and mouse mononuclear phagocyte networks: a tale of two species? *Front Immunol*. 2015;6:330.
44. Haniffa M, Bigley V, Collin M. Human mononuclear phagocyte system reunited. *Semin Cell Dev Biol*. 2015;41:59–69.
45. Ginhoux F, Guilliams M, Naik SH. Editorial: Dendritic cell and macrophage nomenclature and classification. *Front Immunol*. 2016;7:168.
46. Alloatti A, Kotsias F, Magalhaes JG, Amigorena S. Dendritic cell maturation and cross-presentation: timing matters! *Immunol Rev*. 2016;272:97–108.
47. Jakubzick CV, Randolph GJ, Henson PM. Monocyte differentiation and antigen-presenting functions. *Nat Rev Immunol*. 2017;17:349–362.
48. Hamrah P, Liu Y, Zhang Q, Dana MR. The corneal stroma is endowed with a significant number of resident dendritic cells. *Invest Ophthalmol Vis Sci*. 2003;44:581–589.
49. Agarwal V, Bell GW, Nam JW, Bartel DP. Predicting effective microRNA target sites in mammalian mRNAs. *eLife*. 2015;4:e05005.
50. Garcia DM, Baek D, Shin C, Bell GW, Grimson A, Bartel DP. Weak seed-pairing stability and high target-site abundance decrease the proficiency of lsy-6 and other microRNAs. *Nat Struct Mol Biol*. 2011;18:1139–1146.
51. Friedman RC, Farh KK, Burge CB, Bartel DP. Most mammalian mRNAs are conserved targets of microRNAs. *Genome Res*. 2009;19:92–105.
52. Grimson A, Farh KK, Johnston WK, Garrett-Engele P, Lim LP, Bartel DP. MicroRNA targeting specificity in mammals: determinants beyond seed pairing. *Mol Cell*. 2007;27:91–105.
53. Lewis BP, Burge CB, Bartel DP. Conserved seed pairing, often flanked by adenosines, indicates that thousands of human genes are microRNA targets. *Cell*. 2005;120:15–20.
54. Sticht C, De La Torre C, Parveen A, Gretz N. miRWalk: an online resource for prediction of microRNA binding sites. *PLoS One*. 2018;13:e0206239.
55. Raimondi C, Brash JT, Fantin A, Ruhrberg C. NRP1 function and targeting in neurovascular development and eye disease. *Prog Retin Eye Res*. 2016;52:64–83.
56. McKenna CC, Munjaal RP, Lwigale PY. Distinct roles for neuropilin1 and neuropilin2 during mouse corneal innervation. *PLoS One*. 2012;7:e37175.
57. Bouheraoua N, Fouquet S, Marcos-Almaraz MT, Karagogeos D, Laroche L, Chedotal A. Genetic analysis of the organization, development, and plasticity of corneal innervation in mice. *J Neurosci*. 2019;39:1150–1168.
58. Yamazaki R, Yamazoe K, Yoshida S, et al. The semaphorin 3A inhibitor SM-345431 preserves corneal nerve and epithelial integrity in a murine dry eye model. *Sci Rep*. 2017;7:15584.
59. Lee PS, Gao N, Dike M, et al. Opposing effects of neuropilin-1 and -2 on sensory nerve regeneration in wounded corneas: role of Sema3C in ameliorating diabetic neurotrophic keratopathy. *Diabetes*. 2019;68:807–818.
60. Omoto M, Yoshida S, Miyashita H, et al. The semaphorin 3A inhibitor SM-345431 accelerates peripheral nerve regeneration and sensitivity in a murine corneal transplantation model. *PLoS One*. 2012;7:e47716.
61. Wienholds E, Kloosterman WP, Miska E, et al. MicroRNA expression in zebrafish embryonic development. *Science*. 2005;309:310–311.
62. Weston MD, Pierce ML, Rocha-Sanchez S, Beisel KW, Soukup GA. MicroRNA gene expression in the mouse inner ear. *Brain Res*. 2006;1111:95–104.
63. Geng R, Furness DN, Muraleedharan CK, et al. The microRNA-183/96/182 cluster is essential for stereociliary bundle formation and function of cochlear sensory hair cells. *Sci Rep*. 2018;8:18022.
64. Fan J, Jia L, Li Y, et al. Maturation arrest in early postnatal sensory receptors by deletion of the miR-183/96/182 cluster in mouse. *Proc Natl Acad Sci USA*. 2017;114:E4271–E4280.
65. Mencia A, Modamio-Hoybjor S, Morin M, et al. A mutation in the human miR-96, a microRNA expressed in the inner ear, causes non-syndromic progressive hearing loss. In: *6th Molecular Biology of Hearing and Deafness Conference Proceedings*. London, UK: Wellcome Trust; 2007.
66. Lewis MA, Quint E, Glazier AM, et al. An ENU-induced mutation of miR-96 associated with progressive hearing loss in mice. *Nat Genet*. 2009;41:614–618.
67. Peng C, Li L, Zhang MD, et al. miR-183 cluster scales mechanical pain sensitivity by regulating basal and neuropathic pain genes. *Science*. 2017;356:1168–1171.
68. Pham TL, Kakazu A, He J, Bazan HEP. Mouse strains and sexual divergence in corneal innervation and nerve regeneration. *FASEB J*. 2019;33:4598–4609.
69. Hanamsagar R, Alter MD, Block CS, Sullivan H, Bolton JL, Bilbo SD. Generation of a microglial developmental index in mice and in humans reveals a sex difference in maturation and immune reactivity. *Glia*. 2017;65:1504–1520.
70. Loram LC, Sholar PW, Taylor FR, et al. Sex and estradiol influence glial pro-inflammatory responses to lipopolysaccharide in rats. *Psychoneuroendocrinology*. 2012;37:1688–1699.
71. Crain JM, Nikodemova M, Watters JJ. Expression of P2 nucleotide receptors varies with age and sex in murine brain microglia. *J Neuroinflammation*. 2009;6:24.
72. Ballantyne C, Cushman M, Psaty B, et al. Collaborative meta-analysis of individual participant data from observational studies of Lp-PLA2 and cardiovascular diseases. *Eur J Cardiovasc Prev Rehabil*. 2007;14:3–11.
73. Guneykaya D, Ivanov A, Hernandez DP, et al. Transcriptional and translational differences of microglia from male and female brains. *Cell Rep*. 2018;24:2773–2783.e6.
74. Villa A, Gelosa P, Castiglioni L, et al. Sex-specific features of microglia from adult mice. *Cell Rep*. 2018;23:3501–3511.
75. Villa A, Della Torre S, Maggi A. Sexual differentiation of microglia. *Front Neuroendocrinol*. 2019;52:156–164.

Investigative Ophthalmology & Visual Science

76. Schwarz JM, Bilbo SD. Sex, glia, and development: interactions in health and disease. *Horm Behav*. 2012;62:243–253.
77. Jaillon S, Berthenet K, Garlanda C. Sexual Dimorphism in Innate Immunity. *Clin Rev Allergy Immunol*. 2019;56:308–321.
78. Billi AC, Kahlenberg JM, Gudjonsson JE. Sex bias in autoimmunity. *Curr Opin Rheumatol*. 2019;31:53–61.
79. Liang Y, Tsoi LC, Xing X, et al. A gene network regulated by the transcription factor VGLL3 as a promoter of sex-biased autoimmune diseases. *Nat Immunol*. 2017;18:152–160.
80. Ko JA, Mizuno Y, Yanai R, Chikama T, Sonoda KH. Expression of semaphorin 3A and its receptors during mouse corneal development. *Biochem Biophys Res Commun*. 2010;403:305–309.
81. Tanelian DL, Barry MA, Johnston SA, Le T, Smith GM. Semaphorin III can repulse and inhibit adult sensory afferents in vivo. *Nat Med*. 1997;3:1398–1401.
82. Lwigale PY, Bronner-Fraser M. Lens-derived semaphorin3a regulates sensory innervation of the cornea. *Dev Biol*. 2007;306:750–759.
83. Lwigale PY, Bronner-Fraser M. Semaphorin3A/neuropilin-1 signaling acts as a molecular switch regulating neural crest migration during cornea development. *Dev Biol*. 2009;336:257–265.
84. Reza JN, Gavazzi I, Cohen J. Neuropilin-1 is expressed on adult mammalian dorsal root ganglion neurons and mediates semaphorin3a/collapsin-1-induced growth cone collapse by small diameter sensory afferents. *Mol Cell Neurosci*. 1999;14:317–326.
85. Wanigasekara Y, Keast JR. Nerve growth factor, glial cell line-derived neurotrophic factor and neurturin prevent semaphorin 3A-mediated growth cone collapse in adult sensory neurons. *Neuroscience*. 2006;142:369–379.
86. Kubilus JK, Linsenmayer TF. Developmental guidance of embryonic corneal innervation: roles of semaphorin3a and Slit2. *Dev Biol*. 2010;344:172–184.